Synthesis and Characterization of a Series of Novel Heptanuclear Trigonal-Prismatic Polyhedra with Different Edge-Ligands

Jian-Jun Zhang,[a] Sheng-Min Hu,[a] Li-Min Zheng,[b] Xin-Tao Wu,*[a] Zhi-Yong Fu,[a] Jing-Cao Dai,[a] Wen-Xin Du,[a] Han-Hui Zhang,[c] and Rui-Qing Sun[c]

Abstract: Five novel heptanuclear trigonal-prismatic polyhedra, $Na_4[PrNi_6(Gly)_9(\mu_3\text{-}OH)_3(H_2O)_6]\cdot(ClO_4)_7$ (**1**), $Na_2[PrNi_6(Gly)_8(\mu_3\text{-}OH)_3(\mu_2\text{-}OH_2)(H_2O)_6]\cdot(ClO_4)_6\cdot(H_2O)_2$ (**2**), $Na[DyNi_6(Gly)_7(\mu_3\text{-}OH)_3(\mu_2\text{-}OH_2)_2(H_2O)_6]\cdot(ClO_4)_6\cdot H_2O$ (**3**), $[SmNi_6(Gly)_6(\mu_3\text{-}OH)_3Cl_3(H_2O)_6]\cdot Cl_3\cdot(H_2O)_9$ (**4**), and $[ErNi_6(Gly)_6(\mu_3\text{-}OH)_3Cl_3(H_2O)_6]\cdot Cl_3\cdot(H_2O)_9$ (**5**), were synthesized through self-assembly and characterized by X-ray structure analysis. Complex **1** crystallizes in the trigonal *P3* space group ($a = b = 18.1121(2)$, $c = 11.987(0)$ Å, and $Z = 2$). Complex **2** belongs to the triclinic $P\bar{1}$ space group ($a = 16.0145(3)$, $b = 20.58650(10)$, $c = 20.8452(3)$ Å, $\alpha = 78.0590(10)$, $\beta = 67.9200(10)$, $\gamma = 68.1540(10)^\circ$, and $Z = 4$). Complex **3** belongs to the monoclinic *P2(1)/m* space group ($a = 14.9863(3)$, $b = 13.533$, $c = 15.6171(3)$ Å, $\beta = 116.8970(10)^\circ$, and $Z = 2$). Complexes **4** and **5** are isomorphous (**4**: trigonal, $P\bar{3}$; $a = b = 11.8661(4)$, $c = 18.2034(10)$ Å, $Z = 2$; **5**: $a = b = 11.9001(5)$, $c = 18.1229(11)$ Å, $Z = 2$). A Ln^{3+} ion is in the center of the prism formed by six nickel atoms. It coordinates to nine oxygen atoms. Its coordination polyhedron may be best described as a tricapped trigonal prism. The five complexes all have a core of $[LnNi_6(Gly)_6(\mu_3\text{-}OH)_3(H_2O)_6]^{6+}$ and were obtained through the edge-ligand exchange of the three μ_2-OH_2 ligands of $[LnNi_6(Gly)_6(\mu_3\text{-}OH)_3(H_2O)_6(\mu_2\text{-}OH_2)_3]^{6+}$ partly or wholly by glycine or Cl^-. Magnetic measurements reveal that **1** and **4** exhibit antiferromagnetic interaction, while **5** exhibits a ferromagnetic interaction.

Keywords: cluster compounds · lanthanides · magnetic properties · nickel

Introduction

High-nuclearity metal complexes attract much attention in several fields because of their fascinating structures and interesting optoelectronic, magnetic, and catalytic properties.[1] Thus there is much interest in the design and characterization of high-nuclearity clusters. By proper use of suitable chelating ligands such as pyridones,[2] Schiff bases,[3] oxalato,[4] oximates[5] or oxamides,[6] cyano groups,[7] and carboxylic acids,[8–9] heteropolynuclear clusters of transition metals and rare earth metals may be formed, disregarding the distinct difference in their chemical nature. Until now most of the reported 3d–4f complexes have been focused on Gd–Cu coupling which displays magnetic properties amenable to a rather simple analysis. Reports about other lanthanide or transition metal heteronuclear complexes are rather scarce.[10] Up until now, three heptanuclear 3d–4f clusters with the general formula of LnM_6 (M = transition metal) have been reported. They contain the structural motif of an octahedron ($LnNi_6$),[11] trigonal prism ($LnCu_6$),[12a] or wheel ($LnCu_6$).[12b] The only trigonal-prismatic cluster $LnCu_6$ was reported by Gao et al.[12a] and crystallizes in the highly symmetrical hexagonal *P6₃/m* space group with iminodiacetic acid as ligand. Its structure is similar to that of complex **1** except that no edge ligand participates in coordination. This may be because the Cu^{2+} ion is five-coordinate.

An amino acid may coordinate by means of the carboxylate groups with lanthanide ions and the carboxylate or amino groups with transition metal ions. Over the past two decades, although many rare-earth or transition metal complexes with amino acids have been reported,[13,14] only two of these have focused on a system comprising a transition-metal, a rare-earth metal, and an amino acid.[11a, 15a] Therefore, the design

---

[a] Prof. X.-T. Wu, Dr. J.-J. Zhang, MSc. S.-M. Hu, Z.-Y. Fu, J.-C. Dai, W.-X. Du
State Key Laboratory of Structural Chemistry
Fujian Institute of Research on the Structure of Matter Chinese Academy of Sciences, Fuzhou, Fujian 350002 (P.R. China)
Fax: (+86) 591-371-4946
E-mail: wxt@ms.fjirsm.ac.cn

[b] Prof. L.-M. Zheng
State Key Laboratory of Coordination Chemistry
Coordination Chemistry Institute, Nanjing University, Nanjing 210093 (P.R. China)

[c] Prof. H.-H. Zhang, Dr. R.-Q. Sun
Department of Chemistry
Fuzhou University, Fuzhou, Fujian 350002 (P.R. China)

Supporting information for this article is available on the WWW under http://www.chemeurj.org or from the author.

and synthesis of high-nuclearity clusters of this type has been a challenge.

Recently, our research has been focused on the coordination chemistry of lanthanides and transition metals with amino acids.[15] Herein we report five novel heptanuclear lanthanide-centered trigonal-prismatic clusters formed by self-assembly: $Na_4[PrNi_6(Gly)_9(\mu_3\text{-}OH)_3(H_2O)_6]\cdot(ClO_4)_7$ (**1**); $Na_2[PrNi_6(Gly)_8(\mu_3\text{-}OH)_3(\mu_2\text{-}OH_2)(H_2O)_6]\cdot(ClO_4)_6\cdot(H_2O)_2$ (**2**); $Na[DyNi_6(Gly)_6(\mu_3\text{-}OH)_3(\mu_2\text{-}OH_2)_2(H_2O)_6]\cdot(ClO_4)_6\cdot H_2O$ (**3**); $[SmNi_6(Gly)_6(\mu_3\text{-}OH)_3Cl_3(H_2O)_6]\cdot Cl_3\cdot(H_2O)_9$ (**4**), and $[ErNi_6(Gly)_6(\mu_3\text{-}OH)_3Cl_3(H_2O)_6]\cdot Cl_3\cdot(H_2O)_9$ (**5**). The five complexes have a common core of $[LnNi_6(Gly)_6(\mu_3\text{-}OH)_3(H_2O)_6]^{6+}$ and were obtained through the edge-ligand exchange of the three $\mu_2\text{-}OH_2$ ligands of $[LnNi_6(Gly)_6(\mu_3\text{-}OH)_3(H_2O)_6(\mu_2\text{-}OH_2)_3]^{6+}$ partly or wholly by glycine or Cl^- (as shown in Figure 1). The six nickel atoms form a prism in the center of which is an Ln^{3+} ion that coordinates to nine oxygen atoms. Its coordination polyhedron may best be described as a tri-capped trigonal prism.

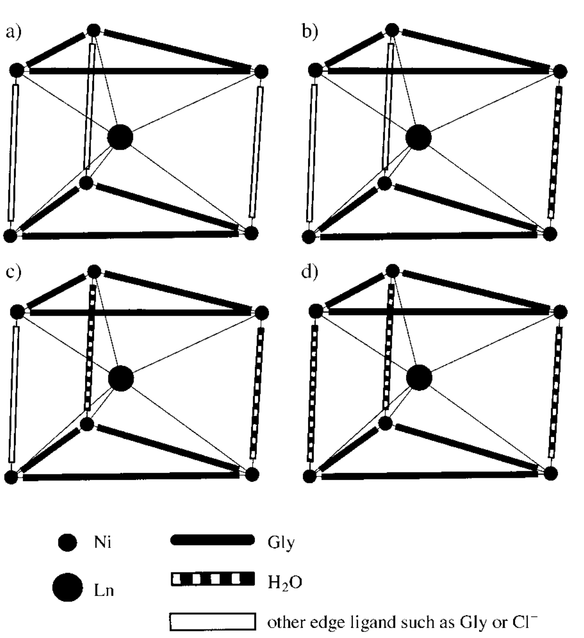

Figure 1. Heptanuclear lanthanide-centered trigonal-prismatic clusters formed through edge-ligand exchange. a) Ln:Ni:Gly = 1:6:9 or Ln:Ni:Gly:Cl^- = 1:6:6:3; b) Ln:Ni:Gly = 1:6:8; c) Ln:Ni:Gly = 1:6:7; d) Ln:Ni:Gly = 1:6:6.

Results and Discussion

Synthesis of the complexes: To date nearly 50 kinds of rare-earth metal complexes with amino acids have been synthesized and structurally characterized.[13] Most of these complexes were synthesized under conditions of pH 1–4. Only three of the reported high-nuclearity rare-earth metal complexes were synthesized under conditions of high pH (pH > 6).[16] There have also been many reports about complexes containing a transition metal and an amino acid in ratios of 1:1 and 1:2 since the 1960s. Most of these complexes were also synthesized at pH 1–4, and had mononuclear, chain, or netted structures.[14] We have synthesized two heptanuclear sodium-centered octahedral copper clusters under conditions of high pH (pH > 6).[15b]

To date there have been only two reports focused on the system comprising a transition metal, a rare-earth metal, and an amino acid, that is the octahedral complex $[LnNi_6(Pro)_{12}]$ reported by Yukawa et al.[11a] and the high nuclearity 3d–4f heteronuclear complex $[\{La_6Cu_{26}(Gly)_{18}(\mu_3\text{-}OH)_{30}(H_2O)_{24}\text{-}(ClO_4)\}(ClO_4)_{21}\cdot(H_2O)_{26}]_n$ reported by our group.[15a] The difficulty of obtaining this kind of complex may be attributed to the fact that rare-earth metal ions and transition-metal ions have distinct differences in their chemical nature, as well as the easy hydrolysis of metal ions under high pH. The design and synthesis of high-nuclearity clusters of this system therefore presents a challenge. By controlling the reactant ratio and the pH value to about 6.6, a series of novel heptanuclear trigonal-prismatic clusters were obtained through the edge-ligand exchange of the three $\mu_2\text{-}OH_2$ ligands of $[LnNi_6(Gly)_6(\mu_3\text{-}OH)_3(H_2O)_6(\mu_2\text{-}OH_2)_3]^{6+}$ partly or wholly by glycine or Cl^- (see Figure 1). Many attempts to synthesize the mother complex $[LnNi_6(Gly)_6(\mu_3\text{-}OH)_3(H_2O)_6(\mu_2\text{-}OH_2)_3]^{6+}$, unfortunately failed; rapid deliquescence prevented it from being structurally characterized.

The structure of complex 1: The structure of the cation is shown in Figure 2, and selected bond lengths and bond angles are given in Table 1. It can be seen from Figure 2 that six Ni^{2+} ions form a large trigonal prism with a Pr^{3+} ion in the center (as shown in Figure 1 a). The distance between the two parallel layers, each of which is composed of three Ni^{2+} ions, is about 3.6 Å. The two Ni^{2+} ions in the corresponding sites are connected by a glycine molecule, which forms the "edge" of the prism. In each layer, the three Ni^{2+} ions form an equilateral triangle, the edges of which comprise a molecule of glycine; the Ni⋯Ni length is about 5.3 Å. The nickel

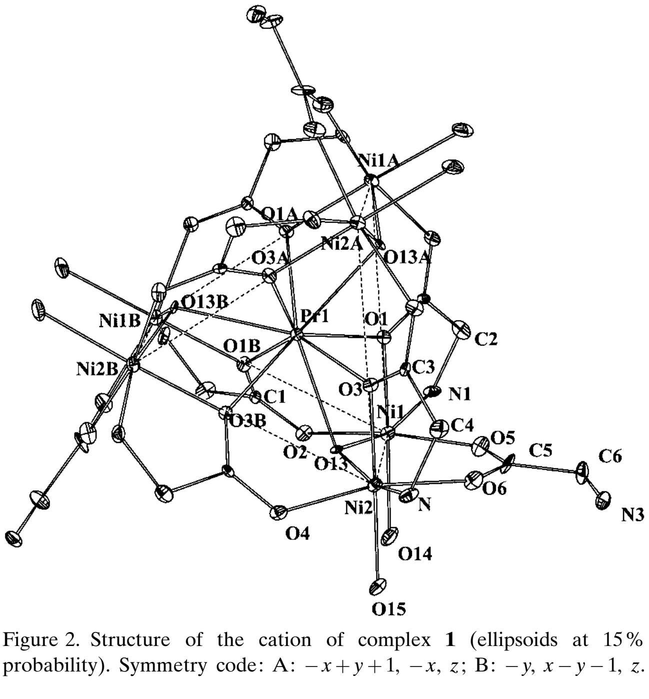

Figure 2. Structure of the cation of complex **1** (ellipsoids at 15% probability). Symmetry code: A: $-x+y+1$, $-x$, z; B: $-y$, $x-y-1$, z.

Table 1. Selected bond lengths [Å] and bond angles [°] for **1**.

Pr1–O1	2.474(8)	Ni1–N1	2.053(11)
Pr1–O3	2.476(8)	Ni2–O3	2.055(9)
Pr1–O13	2.523(8)	Ni2–O4	2.087(10)
Ni1–O1	2.053(9)	Ni2–O6	2.029(11)
Ni1–O2	2.077(10)	Ni2–O13	2.026(8)
Ni1–O5	2.043(11)	Ni2–O15	2.160(13)
Ni1–O13	2.026(8)	Ni2–N2	2.051(11)
Ni1–O14	2.170(13)		
O1A-Pr1-O1	73.2(3)	O3A-Pr1-O3B	73.0(3)
O1A-Pr1-O1B	73.2(3)	O3-Pr1-O3B	73.0(3)
O1-Pr1-O1B	73.2(3)	O13A-Pr1-O13B	120.000(1)
O1A-Pr1-O3A	93.1(3)	O1-Ni1-N1	80.1(4)
O1-Pr1-O3A	139.7(3)	N2-Ni2-O3	80.0(4)
O1A-Pr1-O3	139.8(3)	Ni1-O1-Pr1	103.7(3)
O1-Pr1-O3	93.1(3)	Ni2-O3-Pr1	103.4(3)
O3A-Pr1-O3	73.0(3)	Ni2-O13-Ni1	125.4(4)
O1A-Pr1-O3B	139.7(3)	Ni2-O13-Pr1	102.7(3)
O1B-Pr1-O3B	93.1(3)	Ni1-O13-Pr1	102.8(3)
O1-Pr1-O3B	139.8(3)	O3-Pr1-O13	66.4(3)

Symmetry transformations used to generate equivalent atoms: A: $-x+y+1, -x, z$; B: $-y, x-y-1, z$.

framework may be described as a "flat" equilateral trigonal prism.

The Pr⋯Ni length is about 3.57 Å, which is slightly longer than the Tb⋯Cu length of 3.45 Å in another heptanuclear trigonal prism, $TbCu_6$.[12a] Here, the iminodiacetic acid is the ligand, and the Sm⋯Ni length is 3.7 Å in the heptanuclear octahedron, $SmNi_6$,[11a] which contains proline as the ligand. Short distances may cause strong magnetic exchanges between the 3d and 4f ions.

The coordination polyhedron of the nine-coordinate Pr^{3+} ion (Figure 3) may best be described as a tricapped trigonal prism. The six carboxyl oxygen atoms from six glycine molecules form six apexes, and the three oxygen atoms from three μ_3-OH^- groups form three caps. The Pr–O (prism) bond lengths are about 2.47 Å, which are slightly shorter than the Pr–O (cap) bond lengths (2.52 Å). The distance between the two apexes in the same layer is about 2.95 Å, but the distance between the corresponding two apexes in different layers is about 3.6 Å. The coordination polyhedron may therefore be described as a "prolonged" equilateral trigonal prism.

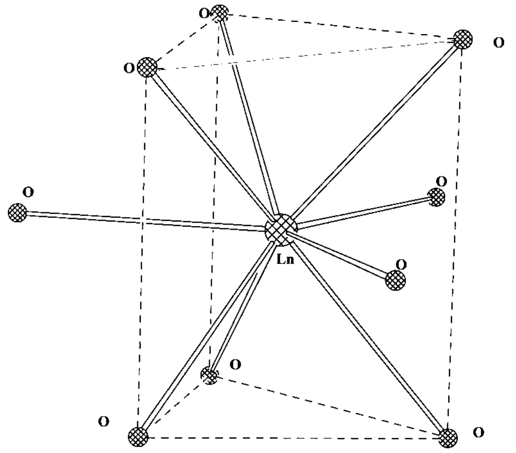

Figure 3. Coordination polyhedron of an Ln^{3+} ion in the clusters.

Each Ni atom has an NO_5 donor set which consists of one nitrogen atom of glycine, three carboxyl oxygen atoms from three glycine ligands, one coordinated water molecule, and a μ_3-OH^- group. The distance from the Ni^{2+} ion to the coordinated water molecule is about 2.17 Å, slightly longer than other Ni–O lengths (about 2.05 Å). The Ni–N lengths are about 2.05 Å. At Ni2 (see Figure 2), small deviations from bond angles of 180° of the idealized octahedral geometry are found (O6-Ni2-O4 166.3(4), O3-Ni2-O15 176.2(4), O13-Ni2-N2 163.9(4)°), implying that all the Ni ions have a slightly distorted octahedral configuration. It should be noted that N3 was found to be disordered.

Each cation has three μ_3-OH^- groups. They are located in the same plane as the Pr^{3+} ion, forming an equilateral triangle with a side length of about 4.37 Å. Each μ_3-OH^- group coordinates to the Pr^{3+} ion and the two corresponding Ni^{2+} ions from the two parallel layers. The O3-Pr1-O13 angle is 66.4(3)° and the Ni2-O13-Ni1 angle is 125.4(4)°.

There are two coordination modes for the glycine ligands, among which six atoms (N1, N1A, N1B and N2, N2A, N2B) are bound in the η^4-coordination mode and three (N3, N3A, N3B) are attached in the η^2-coordination mode (Scheme 1). Within the five-membered chelate rings, the N-Ni-O moiety formed in the η^4-coordination mode has an angle of about 80°.

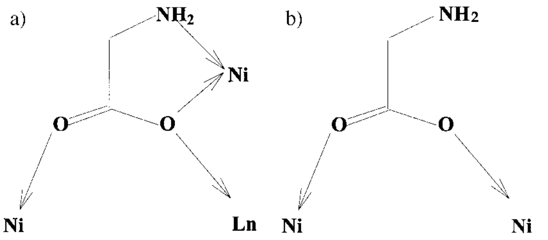

Scheme 1. Two coordination modes of glycine. a) η_4-coordination mode; b) η_2-coordination mode.

The 3D network of complex **1** along the *c* axis is shown in Figure S1 in the Supporting Information. Figure S1 reveals that with the help of the electrovalent bonds between the Na^+ ion and the seven surrounding oxygen atoms, among which are four from the $PrNi_6$ cation and three from the ClO_4^- ions, large honeycomb-like channels may be formed. The Na–O lengths range from 2.3 to 3.0 Å. Figure S2 in the Supporting Information shows a schematic diagram of one of the channels. The side of the big hexagon is about 7 Å and the distance between two layers is about 5.97 Å. Free Na^+ and ClO_4^- ions may be housed in the large channels.

The structure of complex 2: The structure of the cation is shown in Figure 4 and selected bond lengths and bond angles are given in Table 2. The structure is almost the same as that of complex **1** except that only one of the μ_2-H_2O edge ligands is replaced by glycine (see Figure 1b). This causes a slight distortion of the whole structure compared with the highly symmetrical structure of complex **1**. The Ni⋯Ni separations in the same layer are about 5.3 Å, almost the same as that in complex **1**; however, there is some difference in the Ni⋯Ni separations between different layers. When nickel ions are

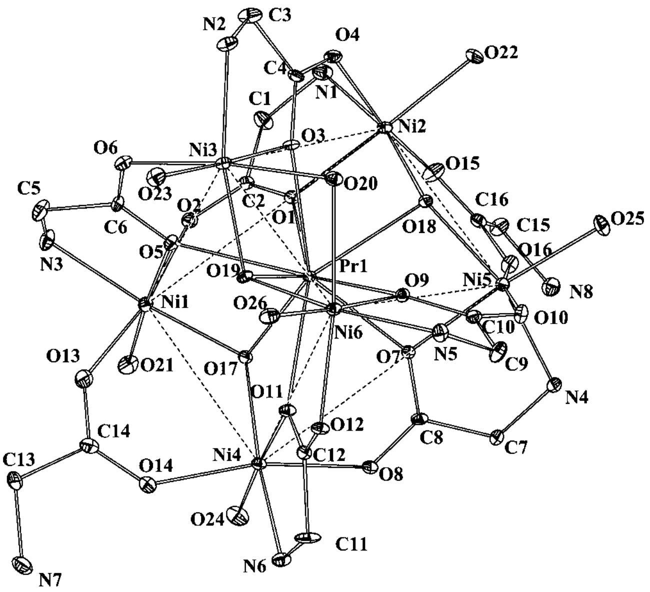

Figure 4. Structure of the cation of complex **2** (ellipsoids at 15% probability).

Table 2. Selected bond lengths [Å] and bond angles [°] for **2**.

Pr1–O1	2.483(6)	Ni3–O23	2.037(7)
Pr1–O3	2.502(6)	Ni3–N2	2.058(9)
Pr1–O5	2.525(6)	Ni3–O6	2.112(7)
Pr1–O7	2.458(6)	Ni3–O20	2.229(7)
Pr1–O9	2.477(6)	Ni4–O14	2.055(8)
Pr1–O11	2.533(6)	Ni4–O17	2.057(6)
Pr1–O17	2.473(6)	Ni4–O11	2.067(6)
Pr1–O18	2.517(6)	Ni4–O8	2.090(7)
Pr1–O19	2.522(6)	Ni4–N6	2.096(8)
Ni1–O17	2.036(6)	Ni4–O24	2.108(7)
Ni1–O13	2.038(9)	Ni5–O18	2.054(6)
Ni1–O21	2.049(7)	Ni5–O25	2.059(7)
Ni1–O5	2.064(7)	Ni5–O16	2.063(7)
Ni1–N3	2.115(9)	Ni5–O7	2.065(6)
Ni1–O2	2.121(7)	Ni5–N4	2.082(8)
Ni2–O18	2.038(6)	Ni5–O10	2.108(7)
Ni2–O15	2.042(8)	Ni6–O19	2.022(6)
Ni2–O22	2.064(7)	Ni6–O9	2.025(6)
Ni2–O1	2.085(7)	Ni6–O26	2.065(7)
Ni2–N1	2.091(9)	Ni6–N5	2.071(8)
Ni2–O4	2.122(7)	Ni6–O12	2.110(6)
Ni3–O19	2.007(6)	Ni6–O20	2.232(7)
Ni3–O3	2.032(7)		
O1-Pr1-O3	76.1(2)	O3-Ni3-N2	81.7(3)
O1-Pr1-O5	71.5(2)	O11-Ni4-N6	80.6(3)
O3-Pr1-O5	71.8(2)	O7-Ni5-N4	81.3(3)
O7-Pr1-O9	76.9(2)	O9-Ni6-N5	82.0(3)
O7-Pr1-O11	75.3(2)	Ni1-O17-Ni4	124.9(3)
O9-Pr1-O11	73.8(2)	Ni1-O17-Pr1	102.1(3)
O17-Pr1-O18	123.4(2)	Ni4-O17-Pr1	103.4(2)
O17-Pr1-O19	112.8(2)	Ni2-O18-Ni5	125.3(3)
O18-Pr1-O19	123.8(2)	Ni2-O18-Pr1	101.7(3)
O5-Pr1-O11	95.6(2)	Ni5-O18-Pr1	102.1(2)
O7-Pr1-O1	93.5(2)	Ni3-O19-Ni6	108.5(3)
O9-Pr1-O3	85.7(2)	Ni3-O19-Pr1	102.3(2)
O5-Ni1-N3	80.4(3)	Ni6-O19-Pr1	101.3(3)
O1-Ni2-N1	80.4(3)	Ni3-O20-Ni6	94.2(2)

connected by a glycine ligand, the Ni···Ni separations are about 3.6 Å, almost the same as that of complex **1**. But when nickel ions are connected by a μ_2-H_2O edge ligand, the Ni···Ni separation is only 3.269 Å. This may lead to the formation of a dihedral angle between the two layers (4.5°).

The nickel atoms have two different coordination environments. Ni1, Ni2, Ni4, and Ni5 have an NO_5 donor set just as in complex **1**. Ni3 and Ni6 also have an NO_5 donor set, but one of the oxygen atoms comes from a μ_2-H_2O group rather than a carboxy group. All the Ni atoms have a slightly distorted octahedral configuration.

The structure of complex 3: Complex **3** crystallizes in the monoclinic system, in the *P*2$_1$/*m* space group. The structure of the complex cation is shown in Figure 5, and selected bond lengths and bond angles are given in Table 3. The structure is almost the same as that of complex **1** except that only two of the edge μ_2-H_2O ligands are replaced by glycine (see Figure 1c). This also causes a slight distortion of the whole structure. The Ni···Ni separation for nickel ions from different layers connected by a glycine edge ligand is 3.654 Å, for those Ni ions connected by a μ_2-H_2O edge ligand the Ni···Ni separations are shorter (Ni1···Ni1A 3.234, Ni2···Ni2A 3.370 Å). This also leads to the formation of a dihedral angle between the two layers (4.5°).

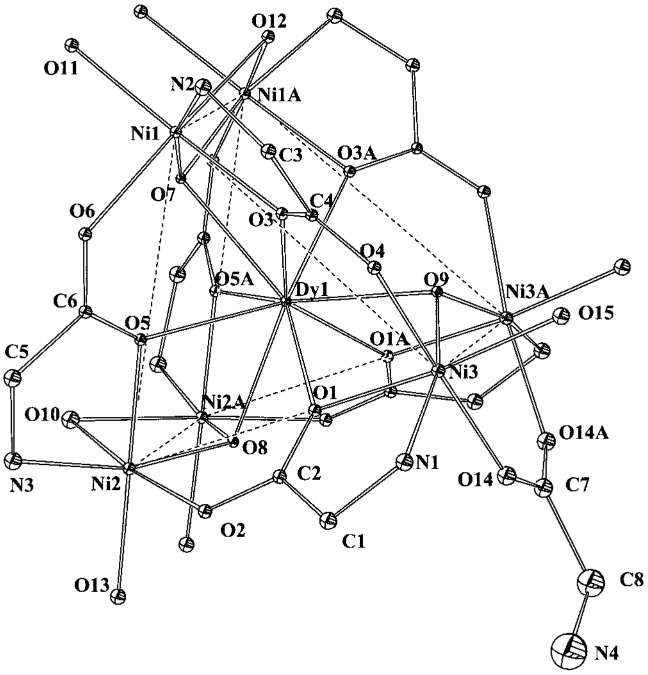

Figure 5. Structure of the cation of complex **3**. Symmetry code: A: *x*, $-y+3/2$, *z*.

The nickel atoms also have two different coordination environments. Ni3 has an NO_5 donor set as in complex **1**, Ni1 and Ni2 also have an NO_5 donor set as in complex **1**, but one of the oxygen atoms comes from a μ_2-H_2O group rather than a carboxy group. All the Ni atoms have a slightly distorted octahedral configuration.

The structure of complexes 4 and 5: Complexes **4** and **5** are isomorphous. The structure of the cation of complex **4** is shown in Figure 6 and selected bond lengths and bond angles

Table 3. Selected bond lengths [Å] and bond angles [°] for **3**.

Dy1–O1	2.445(9)	Ni2–O2	2.086(10)
Dy1–O3	2.455(8)	Ni2–O5	2.060(8)
Dy1–O5	2.484(8)	Ni2–O8	2.010(7)
Dy1–O7	2.480(11)	Ni2–O10	2.316(14)
Dy1–O8	2.440(11)	Ni2–O13	2.083(10)
Dy1–O9	2.431(12)	Ni2–N3	2.080(13)
Ni1–O3	2.040(8)	Ni3–O1	2.065(9)
Ni1–O6	2.128(10)	Ni3–O4	2.142(10)
Ni1–O7	1.996(7)	Ni3–O9	2.061(6)
Ni1–O11	2.059(9)	Ni3–O14	2.059(15)
Ni1–O12	2.223(9)	Ni3–O15	2.083(11)
Ni1–N2	2.087(12)	Ni3–N1	2.106(13)
O1A-Dy1-O1	98.2(5)	O3-Ni1-N2	82.4(4)
O1A-Dy1-O3	140.9(3)	O5-Ni2-N3	81.3(4)
O1-Dy1-O3	75.5(3)	O1-Ni3-N1	81.4(4)
O1-Dy1-O3A	140.9(3)	Ni3-O1-Dy1	102.4(3)
O3-Dy1-O3A	85.6(4)	Ni1-O3-Dy1	102.4(3)
O1-Dy1-O5A	140.1(3)	Ni2-O5-Dy1	100.7(3)
O3-Dy1-O5A	135.2(3)	Ni1-O7-Ni1A	108.2(5)
O1A-Dy1-O5	140.1(3)	Ni1-O7-Dy1	102.9(4)
O1-Dy1-O5	72.9(3)	Ni1A-O7-Dy1	102.9(4)
O3-Dy1-O5	75.8(3)	Ni2A-O8-Ni2	114.0(6)
O3A-Dy1-O5	135.2(3)	Ni2-O8-Dy1	103.7(3)
O5A-Dy1-O5	89.2(4)	Ni3A-O9-Ni3	124.4(6)
O9-Dy1-O8	118.3(4)	Ni3-O9-Dy1	103.0(3)
O9-Dy1-O7	125.5(4)	Ni2-O10-Ni2A	93.4(7)
O8-Dy1-O7	116.2(4)	Ni1A-O12-Ni1	93.3(5)

Symmetry transformations used to generate equivalent atoms: A: $x, -y+3/2, z$.

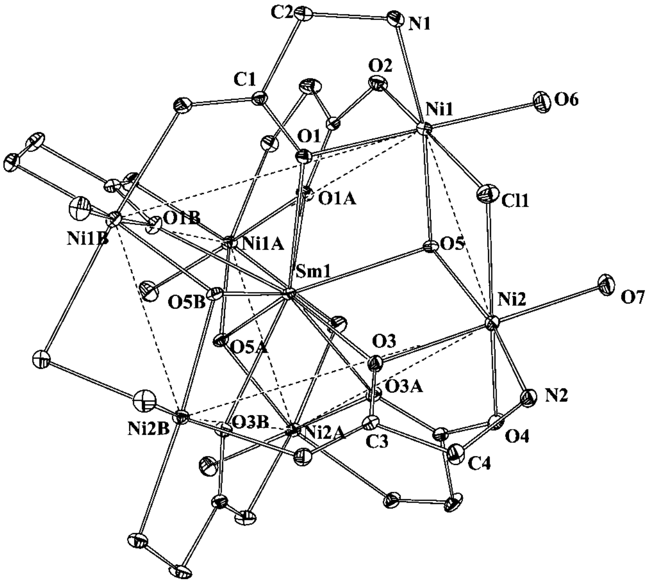

Figure 6. Structure of the cation of complex **4** (ellipsoids at 15% probability). Symmetry code: A: $-y+1, x-y, z$; B: $-x+y+1, -x+1, z$.

Table 4. Selected bond lengths [Å] and bond angles [°] for **4**.

Sm1–O1	2.446(4)	Ni1–Cl1	2.4826(18)
Sm1–O3	2.448(4)	Ni2–O3	2.037(4)
Sm1–O5	2.407(4)	Ni2–O4	2.103(4)
Ni1–O1	2.040(4)	Ni2–O5	2.010(4)
Ni1–O2	2.100(4)	Ni2–O7	2.056(5)
Ni1–O5	2.009(4)	Ni2–N2	2.083(5)
Ni1–O6	2.058(5)	Ni2–Cl1	2.4819(18)
Ni1–N1	2.085(5)		
O5-Sm1-O5A	120.0001	O1-Ni1-N1	80.38(18)
O3A-Sm1-O3	74.15(15)	O3-Ni2-N2	80.47(18)
O1A-Sm1-O1	74.06(16)	Ni1-O1-Sm1	100.37(16)
O5-Sm1-O1	69.57(14)	Ni2-O3-Sm1	100.36(16)
O5B-Sm1-O1A	134.03(14)	Ni1-O5-Ni2	111.6(2)
O5-Sm1-O3	69.54(13)	Ni1-O5-Sm1	102.61(16)
O5-Sm1-O3B	134.14(13)	Ni2-O5-Sm1	102.58(16)
O1-Sm1-O3	91.83(14)	Ni2-Cl1-Ni1	84.10(6)
O1-Sm1-O3A	139.33(13)		

Symmetry transformations used to generate equivalent atoms: A: $-y+1, x-y, z$; B: $-x+y+1, -x+1, z$.

Table 5. Selected bond lengths [Å] and bond angles [°] for **5**.

Er1–O1	2.412(5)	Ni1–Cl1	2.476(2)
Er1–O3	2.412(5)	Ni2–O3	2.046(5)
Er1–O5	2.352(5)	Ni2–O4	2.085(6)
Ni1–O1	2.040(6)	Ni2–O5	2.016(5)
Ni1–O2	2.094(5)	Ni2–O7	2.068(6)
Ni1–O5	2.012(5)	Ni2–N2	2.083(7)
Ni1–O6	2.070(6)	Ni2–Cl1	2.478(2)
Ni1–N1	2.085(7)		
O5-Er1-O5A	120.000(1)	O1-Ni1-N1	81.3(2)
O1A-Er1-O1	74.3(2)	O3-Ni2-N2	81.5(2)
O3A-Er1-O3	74.0(2)	Ni1-O1-Er1	101.1(2)
O5-Er1-O1	69.58(18)	Ni2-O3-Er1	100.9(2)
O5B-Er1-O1A	134.15(18)	Ni1-O5-Ni2	109.8(3)
O5-Er1-O3	69.86(18)	Ni1-O5-Er1	104.0(2)
O5-Er1-O3B	134.12(18)	Ni2-O5-Er1	103.8(2)
O1-Er1-O3	91.73(18)	Ni1-Cl1-Ni2	83.38(7)
O1-Er1-O3A	139.14(18)		

Symmetry transformations used to generate equivalent atoms: A: $-x+y+2, -x+2, z$; B: $-y+2, x-y, z$.

of complexes **4** and **5** are given in Tables 4 and 5, respectively. The structures are almost the same as that of complex **1** except that the three μ_2-H_2O edge ligands are replaced by Cl^- (see Figure 1a). The cluster cation of complex **5** is "smaller" than that of complex **1** because the ionic radius of Er^{3+} is only 0.88 Å, while that of Pr^{3+} is 1.01 Å. From Table 6 we see that the Ni ··· Ni separation in the same layer (ca. 5.24 Å), the Ni ··· Ni separation between different layers (ca. 3.32 Å), the Ln ··· Ni separations (ca. 3.44 Å), and the separation between Ln^{3+} and the two layers (ca. 1.64 Å) for complex **5** are all shorter than those for complex **1** (ca. 5.34, 3.60, 3.57, and 1.8 Å, respectively). Each Ni atom has an NO_4Cl donor set. All the Ni atoms have a slightly distorted octahedral configuration.

The 3D network of complex **4** along the *c* axis is shown in Figure S3 in the Supporting Information. There are weak links between Cl2 and six water molecules (O9), and these six water molecules could form hydrogen bonds with the oxygen atoms (O7) of the $LnNi_6$ clusters. The Cl2–O9 bond length is 3.2 Å and the O9–O7 bond length is 2.86 Å. Weak links help to connect the $LnNi_6$ clusters into honeycomb-like channels. Figure S4 in the Supporting Information shows the schematic diagram of one of these channels. The side of the large hexagon is about 6.85 Å in length and the distance between two layers is about 9.10 Å.

Photoluminescence and magnetic properties: The emission spectra of the five complexes were measured in the solid state at room temperature. (The excitation and emission spectra of compound **1** are shown in Figure S5 in the Supporting Information as an example). It can be observed that all five

Table 6. The comparison of selected bond lengths [Å] and bond angles [°] of the complexes.

	Ni···Ni Separation [Å] (in the same layer)	Ni···Ni Separation [Å] (between different layers)	Ln···Ni Separation [Å]	The separation of Ln^{3+} to the two layers [Å]	The dihedral angle of the two layers [°]	Ni-(μ_2-OH_2)-Ni and Ni-(μ_2-Cl)-Ni [°]
1	Ni1···Ni1A 5.337	Ni1···Ni2 3.600	Pr1···Ni1 3.569 Pr1···Ni2 3.566	1.801 and 1.798	0	–
2	Ni1···Ni2 5.341 Ni1···Ni3 5.257 Ni2···Ni3 5.335 Ni4···Ni5 5.393 Ni4···Ni(6) 5.307 Ni5···Ni(6) 5.346	Ni1···Ni4 3.629 Ni2···Ni5 3.635 Ni3···Ni(6) 3.269	Pr1···Ni1 3.516 Pr1···Ni2 3.546 Pr1···Ni3 3.541 Pr1···Ni4 3.565 Pr1···Ni5 3.568 Pr1···Ni(6) 3.528	1.756 and 1.758	4.5	Ni3-O20-Ni6 94.2
3	Ni1···Ni2 5.308 Ni1···Ni3 5.351 Ni2···Ni3 5.299	Ni1···Ni1A 3.234 Ni2···Ni2A 3.370 Ni3···Ni3A 3.654	Dy1···Ni1 3.512 Dy1···Ni2 3.510 Dy1···Ni3 3.522	1.709	4.5	Ni1-O12-Ni1A 93.3 Ni2-O10-Ni2A 93.4
4	Ni1···Ni1A 5.247 Ni2···Ni2A 5.247	Ni1···Ni2 3.325	Sm1···Ni1 3.456 Sm1···Ni2 3.455	1.663 and 1.662	0	Ni1-Cl1-Ni2 84.1
5	Ni1···Ni1A 5.241 Ni2···Ni2A 5.239	Ni1···Ni2 3.295	Er1···Ni1 3.446 Er1···Ni2 3.444	1.648 and 1.647	0	Ni1-Cl1-Ni2 83.38

complexes exhibit intense photoluminescence emission at about 410 nm ($\lambda_{ex} = 309$ nm) which corresponds to the emission peak of the glycine ligand. No emission peak of the lanthanide metal ion was observed. That the combination of Ni^{2+} or Cu^{2+} ions with the lanthanide ion may lead to the quenching of Ln^{3+} has also been observed by other authors.[17] The reason was proposed to be that energy transfers from the excited Ln^{3+} ion to the Ni^{2+} ions through the bridging oxygen atoms followed by radiationless energy loss.[17]

Temperature-dependent magnetic susceptibilities of complexes **1**, **4**, and **5** were measured in the range 2–300 K (for **1**) or 5–300 K (for **4**, **5**) at 10 kOe. Figure 7 shows the $\chi_M T$ versus T curves for **1** and **4**. At 300 K, the $\chi_M T$ values per $LnNi_6$ unit are 9.46 and 7.93 $cm^3 mol^{-1} K$ for **1** and **4**, respectively, slightly larger than the expected values (9.06 $cm^3 mol^{-1} K$ for **1**, 7.55 $cm^3 mol^{-1} K$ for **4**) for one Ln^{III} free ion and six spin-only Ni^{II} ions ($S = 1$, $g = 2.23$). Upon cooling, the value of $\chi_M T$ decreases continuously for both compounds, suggesting an overall antiferromagnetic coupling. This antiferromagnetic interaction is confirmed by the negative Weiss constants (−16.7 K for **1**, −3.83 K for **4**) determined for data in the temperature range 50–300 K.

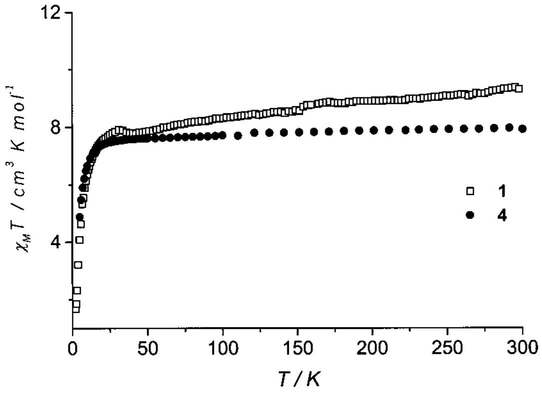

Figure 7. Temperature dependence of magnetic susceptibility of **1** and **4**.

The room temperature $\chi_M T$ value for complex **5** is 18.45 $cm^3 mol^{-1} K$, again in agreement with the calculated value (18.94 $cm^3 mol^{-1} K$) for one Er^{III} free ion and six spin-only Ni^{II} ions (Figure 8). The value of the $\chi_M T$ on cooling remains almost constant down to about 100 K, where it begins to increase smoothly until reaching a maximum of 19.25 $cm^3 mol^{-1} K$ around 28 K. This phenomenon corresponds to an overall ferromagnetic interaction, in contrast to the antiferromagnetic interactions observed in compounds **1** and **4**. Consequently, the Weiss constant determined in the range 50–300 K is +1.07 K for **5**.

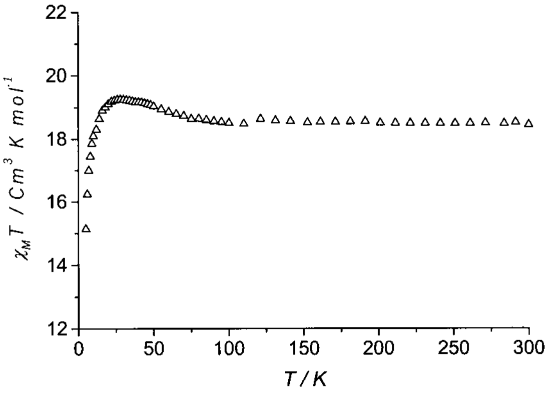

Figure 8. Temperature dependence of magnetic susceptibility of **5**.

According to the structures described above, it is the $LnNi_6$ clusters that make the major contributions to the magnetic behavior of these compounds. Within the $LnNi_6$ core in each case, the Ni–Ni separations in the same layer (5.24–5.39 Å) are much longer than those between the different layers (3.26–3.65 Å) (Table 6). The six Ni atoms can thus be viewed as three Ni_2 dimers, each of which is separated from the others by about 5.3 Å. Considering the length of the Ln–Ni distance in these compounds (3.44–3.57 Å), the magnetic behavior of **1**, **4**, and **5** can be affected by the competitive Ni–Ni (between the different layers) and Ln–Ni interactions, if other factors such as ligand field effects of Ln^{III} are neglected. In compound **1**, the magnetic interaction between Ni1 and Ni2 can be propagated through μ_3-O13 and O5–C5–O6 pathways. The Ni1-O13-Ni2 angle (125.4°) falls in the range where antiferromagnetic exchange is favored for the Ni_2 dimer.[18] The overall antiferromagnetic behavior observed in **1** may indicate that the magnetic interaction of Pr–Ni is also antiferromagnetic.

In compounds **4** and **5**, the Ni1 and Ni2 atoms are bridged by both O5 and Cl1 atoms. The Ni1-O5-Ni2 and Ni1-Cl1-Ni2 angles are 111.6 and 84.1° for **4** and 109.8 and 83.38° for **5**, respectively. Antiferromagnetic coupling should be dominant for the Ni_2 dimers in both cases. The fact that the overall interaction is antiferromagnetic in **4**, while ferromagnetic in **5** suggests that the nature of the interaction between Sm^{III} and Ni^{II} is antiferromagnetic, while that between Er^{III} and Ni^{II} is ferromagnetic. Ferromagnetic coupling was also observed in a similar heptanuclear $TbCu_6$ compound.[12a] Further decreasing of $\chi_M T$ below 28 K in **5** could be due to the antiferromagnetic interactions between the Ni_2 dimers and/or the $ErNi_6$ cores and the ligand field effects of Er^{III} ions.

Conclusion

In summary, a rational synthetic route for the preparation of high-nuclearity clusters of transition-metal/rare-earth metal/amino acid system has been carried out and five heptanuclear trigonal-prismatic clusters have been obtained. Future work will target the synthesis of clusters having other edge ligands such as chiral amino acids and other halogen ions, and clusters in which the ratio of Ln:Ni:Gly is 1:6:6.

Experimental Section

Materials and instrumentation: $Ln(ClO_4)_3 \cdot 6H_2O$ was synthesized by dissolving lanthanide oxide in an excess of perchloric acid. Other starting materials were of reagent grade and were used without further purification. Elemental analyses were carried out by the Elemental Analysis Lab of our Institute. Fluorescence spectra were measured with an Edinburgh FL-FS90 TCSPC system at the Spectroscopy Lab of Fuzhou University. Magnetic measurements were carried out with a Quantum Design PPMS model6000 magnetometer.

Synthesis of the complexes

<+> **$Na_4[PrNi_6(Gly)_9(\mu_3\text{-}OH)_3(H_2O)_6]\cdot(ClO_4)_7$ (1)**: $Ni(ClO_4)_2 \cdot 6H_2O$ (2.184 g, 6 mmol) and glycine (0.675 g, 9 mmol) were added to an aqueous solution (10 mL) of $Pr(ClO_4)_3 \cdot 6H_2O$ (0.546 g, 1 mmol). The pH value of the reaction mixture was carefully adjusted to about 6.6 by slow addition of 0.1M NaOH. After stirring for two hours, the solution was filtered to remove the precipitate and placed in a desiccator filled with phosphorus pentaoxide. Green crystals were obtained about one month later. Elemental analysis calcd (%) for $C_{18}H_{51}Cl_7N_9Na_4Ni_6O_{55}Pr$: C 10.26, H 2.44, N 5.98; found: C 10.16, H 2.63, N 5.58.

$Na_2[PrNi_6(Gly)_8(\mu_3\text{-}OH)_3(\mu_2\text{-}OH_2)(H_2O)_6]\cdot(ClO_4)_6\cdot(H_2O)_2$ (2): The above synthetic procedure was repeated with the exception that the ratio of reactants used was Pr^{3+}:Ni^{2+}:Gly = 1:6:8. Elemental analysis calcd (%) for $C_{16}H_{53}C1_6N_8Na_2Ni_6O_{52}Pr$: C 9.90, H 2.75, N 5.77; found: C 9.36, H 3.13, N 5.31.

$Na[DyNi_6(Gly)_7(\mu_3\text{-}OH)_3(\mu_2\text{-}OH_2)_2(H_2O)_6]\cdot(ClO_4)_6\cdot H_2O$ (3): The above synthetic procedure was repeated with the exception that $Dy(ClO_4)_3 \cdot 6H_2O$ was used and the ratio of reactants was Dy^{3+}:Ni^{2+}:Gly = 1:6:7. Elemental analysis calcd (%) for $C_{14}H_{49}Cl_6DyN_7NaNi_6O_{50}$: C 9.01, H 2.65, N 5.25; found: C 9.10, H 2.63, N 5.27.

$[SmNi_6(Gly)_6(\mu_3\text{-}OH)_3Cl_3(H_2O)_6]\cdot Cl_3\cdot(H_2O)_9$ (4): The above synthetic procedure was repeated with the exception that $Sm(ClO_4)_3 \cdot 6H_2O$ and $NiCl_2 \cdot 6H_2O$ were used and the ratio of reactants was Sm^{3+}:Ni^{2+}:Gly = 1:6:6. Elemental analysis calcd (%) for $C_{12}H_{57}Cl_6N_6Ni_6O_{30}Sm$: C 9.73, H 3.88, N 5.68; found: C 9.44, H 3.67, N 5.43.

$[ErNi_6(Gly)_6(\mu_3\text{-}OH)_3Cl_3(H_2O)_6]\cdot Cl_3\cdot(H_2O)_9$ (5): The above synthetic procedure was repeated with the exception that $Er(ClO_4)_3 \cdot 6H_2O$ and $NiCl_2 \cdot 6H_2O$ were used and the ratio of reactants was Er^{3+}:Ni^{2+}:Gly = 1:6:6. Elemental analysis calcd (%) for $C_{12}H_{57}Cl_6ErN_6Ni_6O_{30}$: C 9.62, H 3.84, N 5.61; found: C 9.36, H 3.69, N 5.36.

X-ray crystallography: Intensity data for the five complexes were collected at 293(2) K on a Siemens Smart/CCD area-detector diffractometer with $Mo_{K\alpha}$ radiation ($\lambda = 0.71073$ Å). Data reductions and cell refinements were performed with Smart-CCD software.[19] An absorption correction by using SADABS software was applied.[20] The structures were solved by direct methods using SHELXS-97[21] and were refined by full-matrix least-squares methods using SHELXL-97. Anisotropic displacement parameters were refined for all non-hydrogen atoms. Final $R = \Sigma \| F_o | - | F_c \| / \Sigma | F_o |$, $R_w = \{\Sigma w[(F_o^2 - F_c^2)^2]/\Sigma w[(F_o^2)^2]\}^{1/2}$, with $w = 1/[\sigma^2(F_o^2) + (aP)^2 + bP]$ [where $P = (F_o^2 + 2F_c^2)/3$]. The crystallographic data are summarized in Table 7. CCDC 184309 – CCDC-184313 contain the supplementary crystallographic data for this paper. These data can be obtained free of charge at www.ccdc.cam.ac.uk/conts/retrieving.html (or from the Cambridge Crystallograghic

Table 7. Crystallographic and data collection parameters for **1**–**5**.

	1	**2**	**3**	**4**	**5**
formula	$C_{18}H_{51}Cl_7N_9Na_4Ni_6O_{55}Pr$	$C_{16}H_{53}C1_6N_8Na_2Ni_6O_{52}Pr$	$C_{14}H_{49}Cl_6DyN_7NaNi_6O_{50}$	$C_{12}H_{57}Cl_6N_6Ni_6O_{30}Sm$	$C_{12}H_{57}Cl_6ErN_6Ni_6O_{30}$
M_r	2106.96	1941.51	1866.05	1480.95	1497.86
crystal system	trigonal	triclinic	monoclinic	trigonal	trigonal
space group	$P3$	$P\bar{1}$	$P2(1)/m$	$P\bar{3}$	$P\bar{3}$
a [Å]	18.1121(2)	16.0145(3)	14.9863(3)	11.8661(4)	11.9001(5)
b [Å]	18.1121(2)	20.58650(10)	13.533	11.8661(4)	11.9001(5)
c [Å]	11.987(0)	20.8452(3)	15.6171(3)	18.2034(10)	18.1229(11)
α [°]	90	78.0590(10)	90	90	90
β [°]	90	67.9200(10)	116.8970(10)	90	90
γ [°]	120	68.1540(10)	90	120	120
V [Å^3]	3405.48(5)	5892.99(14)	2824.77(8)	2219.72(16)	2222.59(19)
Z	2	4	2	2	2
ρ_{calcd} [g cm^{-3}]	2.055	2.188	2.194	2.216	2.238
$F(000)$	2104	3888	1858	1486	1498
measured reflections	11907	29910	9616	6574	5411
independent reflections	7735	20286	5134	2641	2620
R(int)	0.0275	0.0433	0.0477	0.0392	0.0328
goodness of fit on F^2	1.032	1.011	1.175	1.171	1.213
R[a]	0.0796	0.0630	0.0833	0.0414	0.0449
R_w[b]	0.2049	0.1543	0.1794	0.1129	0.1047

[a] $R = \Sigma \| F_o | - | F_c \| / \Sigma | F_o |$; [b] $R_w = \{\Sigma w[(F_o^2 - F_c^2)^2]/\Sigma w[(F_o^2)^2]\}^{1/2}$, $w = 1/[\sigma^2(F_o^2) + (aP)^2 + bP]$, $P = (F_o^2 + 2F_c^2)/3$]. **1**: $a = 0.1274$, $b = 35.9769$; **2**: $a = 0.0960$, $b = 68.6160$; **3**: $a = 0.0439$, $b = 67.7011$; **4**: $a = 0.0512$, $b = 12.7451$; **5**: $a = 0.0397$, $b = 19.5989$.

0947-6539/02/0824-5748 $ 20.00+.50/0

Data Centre, 12 Union Road, Cambridge CB21EZ, UK; fax:(+44)1223-336033; or e-mail: deposit@ccdc.cam.ac.uk).

Acknowledgements

This research was supported by grants from the State Key Laboratory of Structural Chemistry, Fujian Institute of Research on the Structure of Matter, the Chinese Academy of Sciences (CAS), the National Natural Science Foundation of China (NNSFC), and the Science Foundation of CAS and Fujian Province.

[1] a) R. E. P. Winpenny, *Chem. Soc. Rev.* **1998**, *27*, 447–452; b) D. Gatteschi, A. Caneschi, R. Sessoli, A. Cornia, *Chem. Soc. Rev.* **1996**, *25*, 101–109; c) Y. Liang, R. Cao, W. Su, M. Hong, W. Zhang, *Angew. Chem.* **2000**, *112*, 3442–3445; *Angew. Chem. Int. Ed.* **2000**, *39*, 3304–3307; d) H. Yu, W. Zhang, X. Wu, T. Sheng, Q. Wang, P. Lin, *Angew. Chem.* **1998**, *110*, 2662–2664; *Angew. Chem. Int. Ed. Engl.* **1998**, *37*, 2520–2521; e) K, Dimitrou, A. D. Brown, K. Folting, G. Christou, *Inorg. Chem.* **1999**, *38*, 1834–1841.

[2] a) A. J. Blake, R. O. Gould, C. M. Grant, P. E. Y. Milne, S. Parsons, R. E. P. Winpenny, *J. Chem. Soc. Dalton Trans.* **1997**, 1665–1666; b) C. Benelli, A. J. Blake, P. E. Y. Milne, J. M. Rawson, R. E. P. Winpenny. *Chem. Eur. J.* **1995**, *1*, 614–618, and references therein.

[3] a) A. Bencini, C. Benelli, A. Caneschi, R. L. Carlin, A. Dei, D. Gatteschi, *J. Am. Chem. Soc.* **1985**, *107*, 8128–8136; b) J.-P. Costes, F. Dahan, A. Dupuis, *Inorg. Chem.* **2000**, *39*, 165–168; c) J.-P. Costes, F. Dahan, A. Dupuis, *Inorg. Chem.* **2000**, *39*, 5994–6000; d) Q.-Y. Chen, Q.-H. Luo, Z.-L. Wang, J.-T. Chen, *Chem. Commun.* **2000**, 1033–1034; e) M. Sassaki, K, Manseki, H, Horiuchi, M, Kumagai, M. Sakamoto, H. Sakiyama, Y, Nishida, Y. Sadaoka, M. Ohba, H. Okawa, *J. Chem. Soc. Dalton Trans.* **2000**, 259–263.

[4] a) N. Sakagami, K. Okamoto, *Chem. Lett.* **1998**, 201–202; b) S. Decurtins, M. Gross, H. W. Schmalle, S. Ferlay, *Inorg. Chem.* **1998**, *37*, 2443–2449.

[5] a) A. D. Cutland, R. G. Malkani, J. W. Kampf, V. L. Pecoraro, *Angew. Chem.* **2000**, *112*, 2801–2803; *Angew. Chem. Int. Ed. Engl.* **2000**, *39*, 2689–2692; b) M. L. Kahn, C. Mathoniere, O. Kahn, *Inorg. Chem.* **1999**, *38*, 3692–3697; b) M. L. Kahn, M. Verelst, M. Lecantes, C. Mathoniere, O. Kahn, *Eur. J. Inorg. Chem.* **1999**, 527–531.

[6] T. Sanada, T, Suzuki, S, Kaizaki, *J. Chem. Soc. Dalton Trans.* **1998**, 959–965.

[7] a) B.-Q. Ma, S. Gao, G. Su, G.-X. Xu, *Angew. Chem.* **2001**, *113*, 448–451; *Angew. Chem. Int. Ed. Engl.* **2001**, *40*, 434–437; b) K.Harada, J. Yuzurihara, Y. Ishii, N,Sato, H. Kambayashi, Y. Fukuda, *Chem. Lett.* **1995**, 887–888.

[8] a) X.-M. Chen, Y.-L. Wu, Y.-Y. Yang, S. M. J. Aubin, D. N. Hendrickson, *Inorg. Chem.* **1998**, *37*, 6186–6191; b) Y.-Y. Yang, Y.-L. Wu, L.-S. Long, X.-M. Chen, *J. Chem. Soc. Dalton Trans.* **1999**, 2005–2008; c) Y. Cui, G. Cheng, J. Ren, Y.-T. Qian, J.-S. Huang, *Inorg. Chem.* **2000**, *39*, 4165–4168.

[9] R. A. Reynolds, D. Coucouvanis, *J. Am. Chem. Soc.* **1998**, *120*, 209–210.

[10] a) C. Benelli, M. Murries, S. Parsons, R. E. P. Winpenny, *J. Chem. Soc. Dalton Trans.* **1999**, 4125–4126; b) B.-Q. Ma, S. Gao, O. Bai, H.-L. Sun, G.-X. Xu, *J. Chem. Soc. Dalton Trans.* **2000**, 1003–1004, and references therein; c) J.-P. Costes, F. Dahan, B. Donmadieu, J. Garcia-Tojal, J.-P. Laurent. *Eur. J. Inorg. Chem.* **2001**, 363–365; d) R. W. Saalfrank, V. Seitz, F. W. Heinemann, C. Gobel, R. Herbst-Irmer, *J. Chem. Soc. Dalton Trans.* **2001**, 599–603; e) Md. A. Subhan, T. Suzuki, S. Kaizaki, *J. Chem. Soc. Dalton Trans.* **2001**, 492–497; f) Z. Xu, P. W. Read, D. E. Hibbs, M. B. Hursthouse, K. M. Abdul Malik, B. O. Patrick, S. J. Retting, M. Seid, P. A. Summers, M. Pink, R. C. Thompson, C. Orvig, *Inorg. Chem.* **2000**, *39*, 508–516.

[11] a) Y. Yukawa, S. Igarashi, A. Yamano, S. Sato. *Chem. Commun.* **1997**, 711–712; b) D. M. J. Doble, C. H. Benison, A. J. Blake, D. Fenska, M. S. Jackson, R. D. Kay, W.-S. Li, M. Schroder, *Angew. Chem.* **1999**, *111*, 2042–2045; *Angew. Chem. Int. Ed. Engl.* **1999**, *38*, 1915–1918.

[12] a) Q.-D. Liu, S. Gao, J.-R. Li, Q.-Z. Zhou, K.-B. Yu, B.-Q. Ma, S.-W. Zhang, X.-X. Zhang, T.-Z. Jin, *Inorg. Chem.* **2000**, *39*, 2488–2492; b) Y.-J. Zhang, B.-Q. Ma, S. Gao, J.-R. Li, Q.-D. Liu, *J. Chem. Soc. Dalton Trans.* **2000**, 2249–2250.

[13] R. Y. Wang, F. Gao, T.-Z. Jin, *Huaxuetongbao* (Chemistry, in China), **1996**, *10*, 14–20.

[14] a) M. A. A. F. de C. T. Carrondo, M. T. L. S. Duarte, M. L. S. S. Goncalves, P. O'Brien, M. B. Hursthouse, *J. Chem. Soc. Dalton Trans.* **1990**, 213–217; b) J. A. Thich, D. Mastropaoio, J. Potenza, H. J. Schugar, *J. Am. Chem. Soc.* **1974**, *96*, 726–731; c) N. Ohata, H. Masuda, O. Yamauchi, *Angew. Chem.* **1996**, *108*, 570–572; *Angew. Chem. Int. Ed. Engl.* **1996**, *35*, 531–532; d) H. Masuda, A. Odani, T. Yamazaki, T. Yajima, O. Yamauchi, *Inorg. Chem.* **1993**, *32*, 1111–1118.

[15] a) S.-M. Hu, J.-C. Dai, X.-T. Wu, L.-M. Wu, C.-P. Cui, Z.-Y. Fu, M.-C. Hong, Y.-C. Liang, *J. Cluster Science* **2002**, *13*, 33–41; b) S.-M. Hu, W.-X. Du, J.-C. Dai, L.-M. Wu, C.-P. Cui, Z.-Y. Fu, X.-T. Wu, *J. Chem. Soc. Dalton Trans.* **2001**, 2963–2964.

[16] a) B.-Q. Ma, D.-S. Zhang, S. Gao, T.-Z. Jin, C.-H. Yan, G.-X. Xu, *Angew. Chem.* **2000**, *112*, 3790–3792; *Angew. Chem. Int. Ed. Engl.* **2000**, *39*, 3644–3646; b) R. Wang, Z. Zheng, T. Jin, R. J. Staples, *Angew. Chem.* **1999**, *111*, 1927–1930; *Angew. Chem. Int. Ed. Engl.* **1999**, *38*, 1813–1815; c) B.-Q. Ma, D.-S. Zhang, S. Gao, T.-Z. Jin, C.-H. Yan, *New J. Chem.* **2000**, *24*, 251–252.

[17] a) M. Sakamoto, K. Yamamoto, A. Matsumoto, Y. Nishida, H. Okawa, *Bull. Chem. Soc. Jpn.* **1994**, *67*, 2707–2711; b) Q.-Y. Chen, Q.-H. Luo, X.-L. Hu, M.-C. Shen, J.-T. Chen, *Chem. Eur. J.* **2002**, *8*, 3984–3990.

[18] A. P. Ginsberg, *Inorg. Chim. Acta*, **1971**, *5*, 45–68 and references therein.

[19] a) XSCANS (Version 2.1), Siemens Analytical X-Ray Instruments Inc., Madison, WI, 1994. b) G. M. Sheldrick, Program for Empirical Absorption Correction of Area Detector Data, University of Göttingen, 1996.

[20] G. M. Sheldrick, SHELXS-97, Program for X-ray Crystal Structure Solution; University of Göttingen: Göttingen, Germany, **1997**.

[21] G. M. Sheldrick, SHELXL-97, Program for X-ray Crystal Structure Refinement; University of Göttingen: Göttingen, Germany, **1997**.

Received: April 26, 2002
Revised: August 21, 2002 [F4050]